Anal Bioanal Chem
DOI 10.1007/s00216-009-3180-3

ORIGINAL PAPER

Characterization, stoichiometry, and stability of salivary protein–tannin complexes by ESI-MS and ESI-MS/MS

Francis Canon · Franck Paté · Emmanuelle Meudec · Thérèse Marlin · Véronique Cheynier · Alexandre Giuliani · Pascale Sarni-Manchado

Received: 9 June 2009 / Revised: 16 September 2009 / Accepted: 21 September 2009

Abstract Numerous protein–polyphenol interactions occur in biological and food domains particularly involving proline-rich proteins, which are representative of the intrinsically unstructured protein group (IUP). Noncovalent protein–ligand complexes are readily detected by electrospray ionization mass spectrometry (ESI-MS), which also gives access to ligand binding stoichiometry. Surprisingly, the study of interactions between polyphenolic molecules and proteins is still an area where ESI-MS has poorly benefited, whereas it has been extensively applied to the detection of noncovalent complexes. Electrospray ionization mass spectrometry has been applied to the detection and the characterization of the complexes formed between tannins and a human salivary proline-rich protein (PRP), namely IB5. The study of the complex stability was achieved by low-energy collision-induced dissociation (CID) measurements, which are commonly implemented using triple quadrupole, hybrid quadrupole time-of-flight, or ion trap instruments. Complexes composed of IB5 bound to a model polyphenol EgCG have been detected by ESI-MS and further analyzed by MS/MS. Mild ESI interface conditions allowed us to observe intact noncovalent PRP–tannin complexes with stoichiometries ranging from 1:1 to 1:5. Thus, ESI-MS shows its efficiency for (1) the study of PRP–tannin interactions, (2) the determination of stoichiometry, and (3) the study of complex stability. We were able to establish unambiguously both their stoichiometries and their overall subunit architecture via tandem mass spectrometry and solution disruption experiments. Our results prove that IB5·EgCG complexes are maintained intact in the gas phase.

Keywords Polyphenol · Interaction · Proline-rich protein · Saliva · Astringency · IUP

Abbreviations

CID	collision-induced dissociation
EgCG	epigallocatechin gallate
ESI	electrospray ionization
IUP	intrinsically unstructured protein
MS	mass spectrometry
MS/MS	tandem mass spectrometry
PRP	proline-rich protein
Q-TOF	quadrupole/time-of-flight

Introduction

Demonstrations of proteins having little or no ordered structure under physiological conditions have increased exponentially over the past 15 years. Particular terms have been proposed to describe these proteins: intrinsically disordered proteins (IDPs), natively unfolded or intrinsically unstructured proteins (IUPs) [1–3]. Proline-rich proteins

F. Canon · F. Paté · E. Meudec · T. Marlin · V. Cheynier · P. Sarni-Manchado (✉)
UMR 1083 Sciences Pour l'Oenologie,
Polyphenol Interaction Research Group, INRA,
Bât 28, 2 place Viala,
F-34060 Montpellier, France
e-mail: sarni@supagro.inra.fr

A. Giuliani
DISCO beamline, Synchrotron Soleil,
l'Orme des Merisiers,
91192 Gif sur Yvette, France

A. Giuliani
CEPIA, INRA,
BP 71627, F-44316 Nantes, France

Published online: 18 October 2009

(PRPs), which are IUPs, are particularly abundant in human saliva and may constitute 70% of total secreted proteins in parotid saliva [4]. The salivary proteins play various roles (e.g., lubrication, digestion, taste, protection) as saliva is the first fluid which interacts with food constituents. Herbivorous and omnivorous mammals have developed the ability to synthesize salivary basic proline-rich proteins whose only known role is to bind tannins [5].

Plants synthesize a diverse group of phenolic compounds (*syn*. polyphenols) [6]. Among them, proanthocyanidins (*syn*. condensed tannins) are ubiquitous in plants and they are major components of foods (e.g., fruit, cocoa), beverages (e.g., wine, tea, beer, cider), animal feeds (e.g., pasture legumes), and herbal remedies. These molecules have attracted considerable interest because of their major contribution to organoleptic and biological properties. One of their prominent characteristics is their ability to interact with proteins, which can be either detrimental or beneficial. For example, haze developments are observed in beverages [7–9], reducing their quality. Inactivation of digestive enzymes and/or tanning of diet proteins impede their digestibility and assimilation, and thus lower nutritional value of some feeds (e.g., legumes) [10]. On the other hand, polyphenol–protein interactions are also involved in the beneficial antioxidant activity of polyphenols as enzyme inhibitors that limit superoxide and uric acid formation [11]. Recently, the participation of polyphenols in the regulation of gene expression, due to their ability to interact with receptors and nuclear factors, has been demonstrated [11].

According to Red Queen hypothesis[1] [12], animals developed shunning mechanisms along with the ability to perceive astringency. Astringency is a tactile sensation [13–16] resulting from interactions of tannins and showing some specificity [17] for which salivary PRPs are often evoked [18]. However, its physicochemical bases are still poorly understood. Protein–tannin interactions have been extensively studied using a variety of techniques and experimental models in relation to astringency and anti-nutritional effects and are reported to generate insoluble and soluble complexes [19–22]. Earlier works have measured protein and/or tannins remaining in solution after precipitation. Particular proteins have been proposed for use in studying protein–polyphenol interactions [23, 24]. However, these measurements may not reflect astringency as salivary protein–tannin interactions show some specificity [17], nor do they take into account the formation of soluble complexes. The first information on the structure of soluble complexes was provided by spectrometric methods such as nuclear magnetic resonance (NMR) [25–28] sometimes in association with molecular modeling [20, 29], circular dichroism (CD) [20, 21], and mass spectrometry [20, 30–32]. However, only peptides have been considered in these studies because of the unavailability of a model of natively unstructured PRPs.

Mass spectrometric procedures have greatly evolved and became methods of choice for characterization of biological macromolecules as well as their interactions. Electrospray ionization (ESI) has been demonstrated to be efficient to probe weak associations of molecules in solution such as receptor–ligand and protein–nucleic acid interactions [33, 34]. ESI-MS offers speed and sensitivity in monitoring components of mixtures. Determination of dissociation or relative binding affinities of noncovalent complexes is now well established [35–37]. The stabilities of noncovalent complexes have been assessed by their resistance to dissociation in the mass spectrometer using collision-induced dissociation (CID) or thermal denaturation experiments [38–40]. Recently, Xie and Loo wrote that "The direct detection of protein–ligand noncovalent complexes using ESI mass spectrometry can be challenging, depending on the types of compounds tested and the types of physical interactions necessary to maintain a stable complex in both solution and in the gas phase." This is certainly one of the reasons why few mass spectrometry publications concern protein–polyphenol complexes. Although these experiments have to be carefully interpreted with regards to solution-phase studies, they can provide information that is difficult to determine otherwise: the contribution of intermolecular interactions to ligand binding, free of any solvent contribution. MS and MS/MS allow one to probe intermolecular interactions experimentally [41].

We report here the first study of noncovalent complexes of the human salivary protein IB5 with tannins by using ESI-MS and MS/MS. IB5 is an intrinsically unstructured proteins of human saliva, whose interactions with tannins may be involved in astringency.

Materials and methods

Samples

Epigallocatechin gallate (EgCG) and reserpine (Fig. 1) were purchased from Sigma (Sigma Chemical Co., Poole, UK).

The human salivary proline-rich protein, IB5, was produced by use of the yeast *Pischia pastoris* as a host organism and purified as previously described [42].

EgCG and protein stock solutions were prepared in water/ethanol (88:12 v/v) acidified to pH 3.1 with acetic acid and were immediately frozen (−20 °C) to prevent

[1] Van Valen's Red Queen hypothesis is a model of coevolution driven by competitive interactions between species. It contrasts with the stationary or 'lost world' model, in which evolution is driven primarily by environmental change.

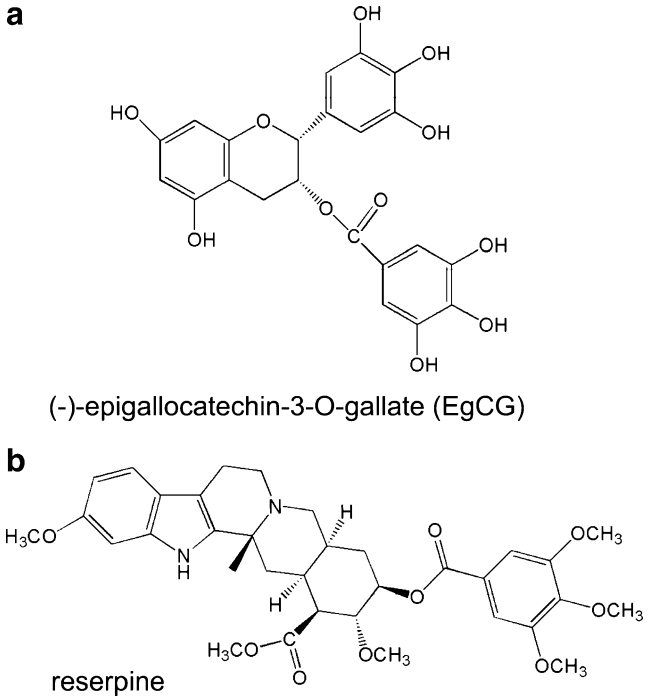

Fig. 1 Structures of **a** epigallocatechin-3-*O*-gallate (EgCG) and **b** reserpine

EgCG oxidation and proteolysis. Before use, they were diluted at room temperature to the desired concentrations.

EgCG–protein interactions

Formation of complexes was studied at pH 3.1, which corresponds to the average pH value of the mouth in the presence of a red wine. For IB5–EgCG interactions, the protein concentration was kept constant at 5 μM in the water/ethanol medium described above. EgCG and protein solutions were mixed extemporaneously at room temperature (regulated at 24 °C) so as to obtain a protein/polyphenol molar ratio of 1:10.

IB5 was mixed with EgCG (final concentration 5 μM and 50 μM, respectively) and allowed to equilibrate at room temperature for at least 5 min before ESI-MS analysis. All samples were prepared in triplicate and analyzed by ESI-MS.

Electrospray ionization mass spectrometry

MS spectra were obtained on a AccuTOF (JEOL, Tokyo, Japan) mass spectrometer equipped with an ESI source and a time-of-flight (TOF) mass analyzer, providing a resolving power of 6,000 at *m*/*z* 609. Each solution was injected into the mass spectrometer by means of a syringe infusion pump at a flow rate of 20 μL min^{-1}. The source voltage was set at 2,350 V in positive ion mode, the orifice 1 voltage at 35 V, the orifice 2 voltage at 5 V, the ring voltage at 10 V, and the capillary temperature at 150 °C. Spectra were acquired in positive ion mode from *m*/*z* 300 to 1,800. Each mass spectrum was acquired with an integration time of 1 s. The signal from 28 scans was accumulated in the multichannel acquisition mode and averaged.

Tandem mass spectrometry

Tandem mass spectrometry experiments were performed on a hybrid quadrupole time-of-flight (Q-TOF) Qstar Pulsar i mass spectrometer (Applied Biosystems, Forster City, CA), providing a resolving power of 10,000 at *m*/*z* 1,080.8. The Q-TOF was operated with the Turbospray (electrospray ion source). The interface was fitted with the IonCooler Guide to preserve the noncovalent complexes upon transfer into the gas phase. The IonCooler Guide is fitted around the initial ion entrance region of Q0 and increases the local pressure to greater than 30 mTorr, which greatly improves detection of weakly bound complexes [43]. The sample was injected into the mass spectrometer by means of a syringe infusion pump at a flow rate of 7 μL min^{-1}. The source voltage was set to 5,800 V in positive ion mode, the declustering potential at 47 V, the focusing potential at 209 V, the declustering potential 2 at 17 V, the ion source gas 1 set at 22, the ion source gas 2 at 0, the curtain gas at 10, and the capillary was not heated up. Nitrogen from a generator, containing less than 6 ppm oxygen, was used both as nebulizing and desolvation gas. During MS/MS experiments, nitrogen was used as collision gas in the collision cell (Linac) with CAD gas setting of 5. The collision-set energy voltage V_c was increased from 0 to 50 V. The kinetic energy of the precursor ion in the laboratory frame of reference is $E_{Lab} = z \times e \times V_c$, where z is the number of charges on the ion and e is the charge of an electron [44]. Data were acquired by the TOF analyzer at 1 acquisition/s with *m*/*z* ranging from 250 to 1,800.

Analysis of ESI-MS and ESI-MS/MS experiments and calculations

All experiments were repeated at least three times. Ion pattern and intensities were compared. ESI-MS and collision MS/MS data were analyzed with Analyst QS [45] and MagTran [46] software.

A procedure adapted from Jørgensen et al. [47] and Wan et al. [48] was used to establish the dissociation curves. The 50% dissociation energy is defined as the energy giving a 50% loss of precursor complex ions. Based on the data of Akashi et al. [49], one of the multiprotonated molecules of the IB5·EgCG complex (M), $[M+6H]^{6+}$, was selected and submitted to CID.

Results and discussion

ESI analysis of the protein solution

Figure 2a shows a representative positive electrospray ionization spectrum of purified IB5 (5 μM in H_2O/EtOH, 88:12 v/v, pH 3.1). The theoretical average molecular mass (MM) of IB5 is 6,923.74 Da (Table 1). The positive ESI mass spectra of IB5 showed a series of ion peaks from *m*/*z* 1,385 to 630, with charge states ranging from +5 to +11 which was confirmed by TOF-MS analysis (data not shown). Peaks have been assigned to protonated molecules. The IB5 spectrum analysis and deconvolution resulted in three molecular mass values of 6,923.70, 6,642.63, and 6,360.39 Da. It reveals the presence of three sequences of IB5, namely IB5a, IB5b, and IB5c, which correspond respectively to the whole protein and to N-terminal proteins with three and six amino acids (aa) deleted (Fig. 2b), with IB5a being the main form (>65%). Each form of IB5 exhibits the same charge state distribution (CSD). Typical protein purification techniques (and particularly for IUPs [1]) do not allow the separation of proteins with such small differences in length, the overall sequence remaining exactly the same. Edman sequencing experiments confirmed that IB5b and IB5c are not the result of fragmentation during the ionization but coexist in the purified fraction with IB5a. They may result from proteolytic activity of *Pichia pastoris* during protein expression or remaining during the protein purification procedure. It is worth noticing that peaks corresponding to multimers (i.e., aggregates) of IB5 were not observed, consistent with the absence of contribution from nonspecific association under the solution and instrumental conditions selected.

Under acidic conditions, the basic residues Arg, Lys, His and the NH_2 terminus are often the only sites of protonation, but in the gas phase [50, 51], Pro and Gln behave as basic residues that can be protonated. The high charge states observed for IB5 can thus be related to the ability of Pro residues to be easily protonated. Investigations on the effect of pH and organic solvent on the CSD of IB5 performed from pH 2.6 to 5.7 in the experimental medium and at a pH value of 1.3 in acetonitrile/water/TFA (80:20:0.1% v/v) showed no difference in the MS spectra. The natively unfolded nature of IB5 explains these data as evidenced earlier by CD experiments

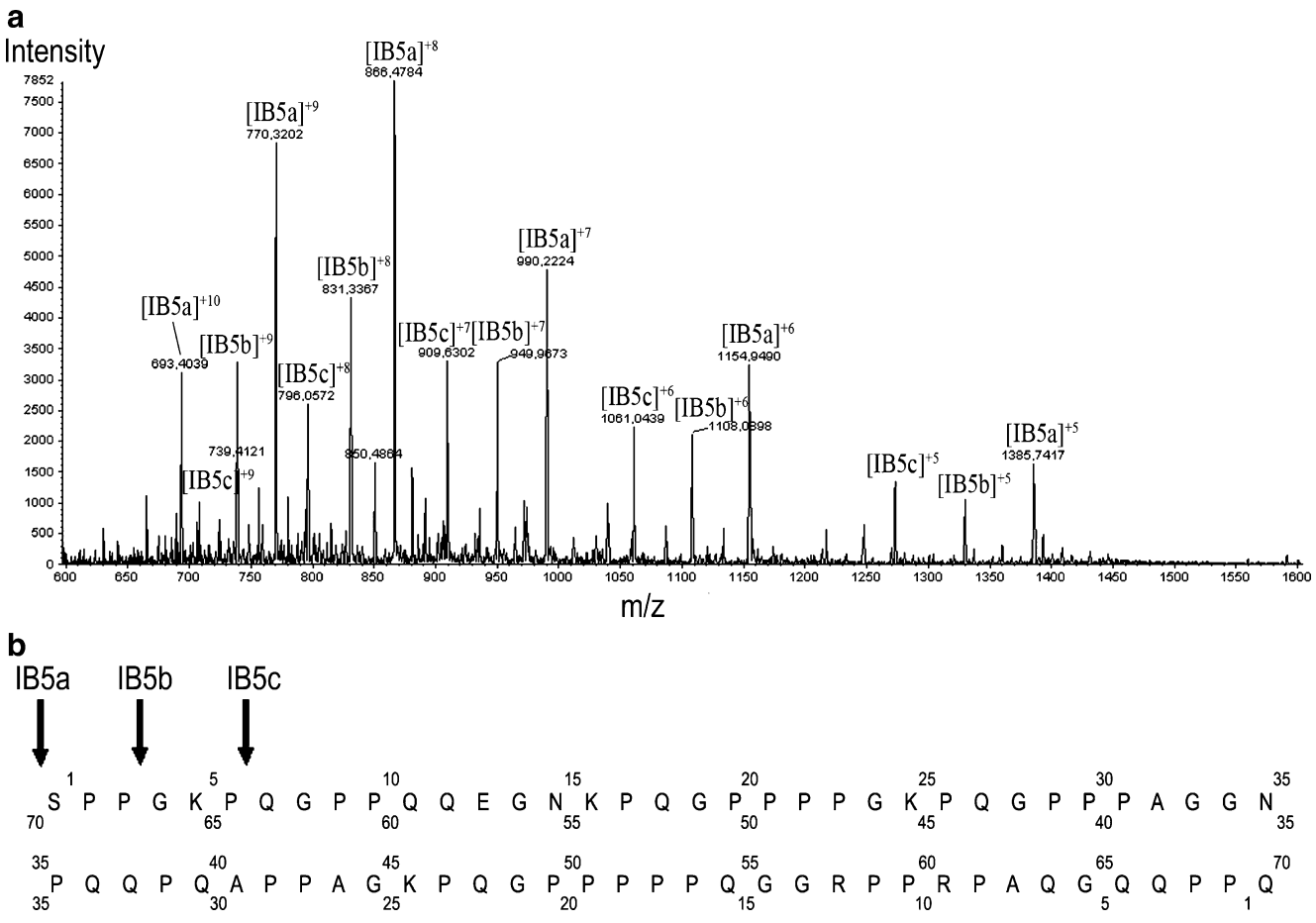

Fig. 2 **a** Positive-ion ESI mass spectrum of salivary PRP IB5 purified from PRPs produced by PRB4S transformant *Pichia pastoris* yeast. **b** Deduced primary sequences of the purified IB5*x*

Table 1 Theoretical and measured mass (Da) of IB5 purified from heterologous *Pichia pastoris*-expressed PRPs

	IB5a	IB5b	IB5c
Theoretical average mass	6,923.74	6,642.43	6,360.08
Measured average mass	6,923.70	6,642.63	6,360.39

[21]. The highest charged ions may represent extensively unfolded solution conformers, whereas the low charge states are assigned to more "compact" series [52].

IB5 fragmentation experiments via CID MS/MS performed on the Q-TOF instrument demonstrated that the highest charged ions were less stable than the lowest charged ones as reported for other proteins and according to the theory of proton mobility [53]. Whereas most investigations on proline-rich sequences under CID have concerned peptides [54, 55], we examined the fragmentation of a whole PRP, IB5, 70-aa long. The ESI-MS/MS spectrum of the $IB5^{7+}$ ion is shown in Fig. 3, which also presents cleavages that occur on the IB5 sequence. The CID spectra of the parent ion are primarily composed of singly, doubly, triply, and some quadruply charged fragments, and the C-terminal y series dominates. The y_{29} and y_{32} ions, corresponding to cleavages on the N-terminal side of proline residues, are the most abundant product ions. The y sequence ions are mainly observed in the center part of the protein backbone. The b_{38}, b_{37}, and b_{35} ions are present with their respective corresponding c ions. Moreover, many internal fragment ions are detected. Their interpretation remains difficult because of repeated sequences and proline abundance in IB5. This protein presents a low-complexity primary sequence, with only 9 different residues, and within the 70 amino acids, 29 are P, 13 are G, and 13 are K, with repeats of KPQGPP(P). P, G, and K residues are interesting from a mass spectrometry point of view [56]. Indeed, the presence of proline in a peptide induces the so-called proline effect which is characterized by the presence of a labile amide bond on the N-terminal side of proline and a stable amide bond on its C-terminal side which is associated with the abundance of y sequence ions [55]. Fragmentation of proline-containing peptides, particularly when poly-Pro stretches exist, produces unusual fragment ions in high-energy experiments, some of which are suggested to be produced by charge-remote cleavage [54]. Complete sequence information cannot be obtained because fragment ions arising from cleavages occurring not adjacent to proline amide bonds have very low abundances or are missing [57].

ESI-MS analysis of IB5·EgCG complexes

Concentrations of condensed tannin in red wine are approximately 1–2 g L^{-1}, corresponding to a mean molar concentration of 0.5–1 mM. In biological media as well as in processing media, polyphenols are often present together with proteins. For example, fining treatment, consisting in the addition of a protein fining agent, is applied to precipitate tannins from plant-derived beverages, so as to decrease haze and/or astringency. Fining agents are gelatin fractions submitted to different hydrolysis leading to different protein sizes. In the case of a red wine, addition of 8–20 g of protein per hectoliter of wine is of general use [58]. Thereby, the concentration of a fining protein showing a 10-kDa apparent MM at 10 g hL^{-1} can be estimated to be around 20 μM. The presence of food in the mouth initiates both mechanical and chemical stimuli via neural reflexes that result in an increased secretion of saliva with taste being the main stimulant for this secretion. Thus, the confrontation between polyphenols and salivary proteins is the first step of ingestion of plant products. The concentration of proteins in saliva is approximately 1 mg mL^{-1}, circa 83 μM. Polyphenols are present in large excess compared with proteins both in wine and in the mouth after sipping of wine, making the protein/polyphenol ratio always in favor of polyphenols. On this basis, to investigate soluble protein–polyphenol complexes we use a protein/polyphenol ratio of 1:10 that does give rise neither to the formation of precipitate nor cloudiness.

Premixed interaction medium with a 1:10 IB5/EgCG molar ratio (5 μM of IB5 with 50 μM of EgCG in H_2O/EtOH, 88:12 v/v, pH 3.1) was introduced into the ESI mass spectrometer. The successful analysis of noncovalent assemblies by MS requires the preservation of the native state of the complex in solution. It is crucial to use aqueous solutions containing only volatile buffers [59]. The MS analysis was performed in water/ethanol, allowing satisfactory levels of desolvation [59]. Analysis of the ESI mass spectrum (Fig. 4a) revealed three distinct entities, IB5, EgCG, and noncovalent soluble complexes in agreement with earlier isothermal titration microcalorimetry (ITC) and CD experiments [21]. It is noteworthy that no indication about their stoichiometries was obtained by other approaches. The CSD of these ions ranged from +6 to +10, like those of individual IB5 proteins. IB5a complexes remain predominant as expected from the protein sample analysis. Figure 4b presents a blowup of the region of the spectrum corresponding to the +7 ions. This is the main charge state for both IB5 and IB5·EgCG complexes. It can be noted that numerous stoichiometries ranging from 1:1 to 1:5 are observed. ESI mass spectra of a mixture of IB5 and reserpine, the latter having a chemical structure with aromatic rings and a molecular mass close to that of EgCG, did not give rise to complex peaks (data not shown). If the interaction is not driven by polyphenols, ESI-MS should have generated complexes between IB5 and reserpine. Use of reserpine allows us to confirm that the formation of complexes is related to tannins.

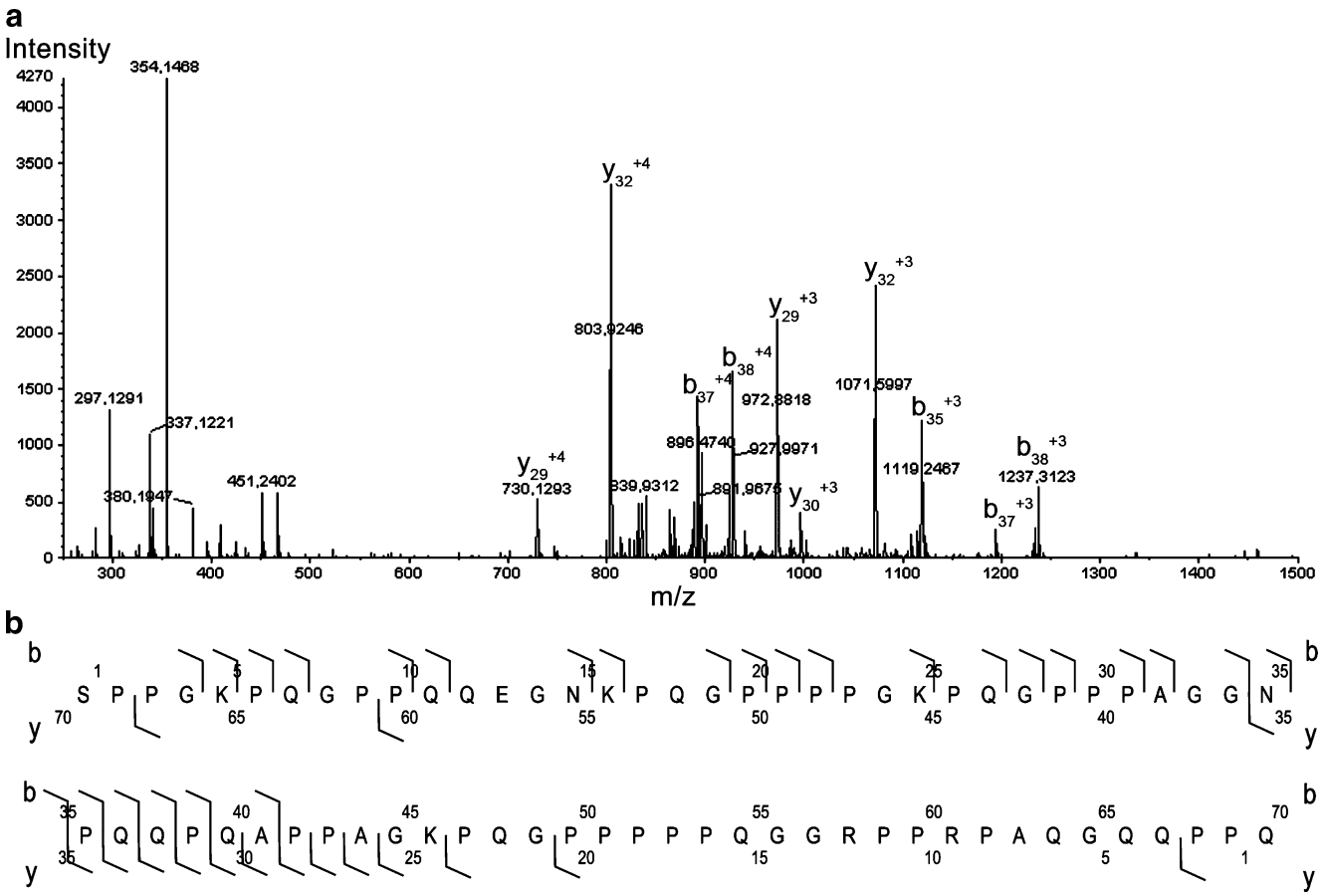

Fig. 3 **a** MS/MS spectrum of product ions obtained by CID of the 7+ charged ion of IB5, collision energy 280 eV. **b** Primary CID fragmentation reactions of IB5

From previous solution studies, proline-rich peptide–tannin interaction involves stacking of the planar proline ring with the phenolic ring, stabilized by hydrogen bonding interactions with the peptide bonds next to the proline and with other amino acids like glycine [20, 26, 60]. Involvement of both enthalpy-driven (attributed to hydrogen bonding) and entropy-driven (associated with the hydrophobic effect and conformational changes) phenomena in interactions of flavan-3-ols with poly-L-proline was confirmed by ITC [61]. The former phenomenon is prevalent in the case of monomers and the latter in that of polymers. Survival of small protein–ligand complexes is largely dictated by the nature of the interaction. In the gas phase, electrostatic and hydrogen bonding interactions are enhanced, whereas hydrophobic interactions are partly or completely lost [62, 63]. Full-scan simple mass spectra with soft ionization conditions obtained in our study probe the composition of the solution and relative abundance of the species. We show that IB5·EgCG complexes are preserved and may involve more than one tannin. The preservation of supramolecular complexes formed by IB5 and EgGC, a model of biological interest with regards to astringency, in the gas phase demonstrates the strength and the contribution of hydrogen bonding [62], in agreement with previous studies using the medium considered here [20]. As previously stated, the main function described for basic salivary PRPs, like IB5, is to be a scavenger which binds tannins [22, 64–66]. Scavenger IUPs function by molecular recognition and often can bind several partners at the same time [67]. Observation of multiple stoichiometries ranging from 1:1 to 1:5 is consistent with IB5's proposed function. Basic PRPs have to bind more than one molecule of tannins to counteract their effects, especially when tannin concentration is rather high.

ESI-MS/MS analysis of IB5·EgCG complexes

Collision-induced dissociation is a process whereby precursor ions are activated upon collision with an unreactive gas, such as argon or nitrogen in the present case. Each collision increases the overall vibrational energy of the molecule until there is enough internal energy accumulated within the molecule to overcome the bond energy, thus causing dissociation [68]. Different cases need to be

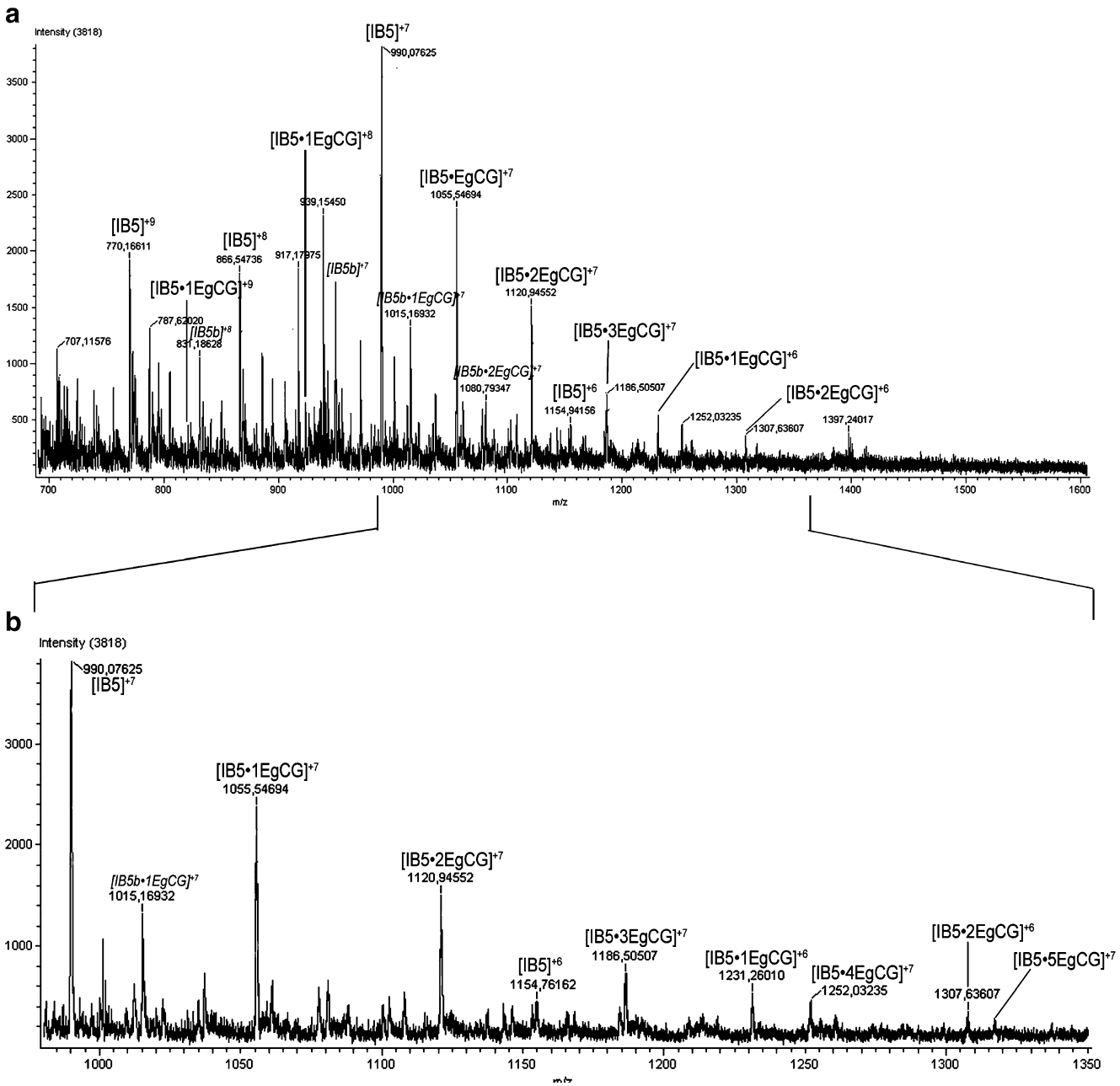

Fig. 4 **a** Positive-ion ESI mass spectrum obtained from mixture of IB5 and EgCG (5 μM:50 μM). **b** Expanded mass region of the 7+ complex ions

considered. Proteins with the lowest charge states are reported to have a conformation close to that in solution [69]. Therefore ESI conditions must be controlled, but also the charge state of the complex ion selected. ESI-MS/MS was performed on IB5·EgCG mixtures. Low-energy CID investigated the relative gas phase stability of the non-covalent IB5·EgCG complexes with 1:1 and 1:2 stoichiometries in the +6 charge state. The same experiments performed on +7 ions gave similar results but IB5 fragmentation was observed. During CID experiments, complex ions are accelerated with voltage offsets up to the 50-V range into the gas-filled collision cell where their translational energy is partly converted into internal energy in a multicollisional process. As mentioned earlier, the kinetic energy of the precursor ion in the laboratory frame of reference is obtained from $E_{\mathrm{Lab}}=z\times e\times V_{\mathrm{c}}$, where z is the number of charges on the ion and e is the charge of an electron [44]. Therefore, the collision energy for the +6 precursor was increased from 0 eV to 300 eV. Collision-induced total dissociation of both complexes (1:1 and 1:2) gave rise to the ions corresponding to $[IB5]^{6+}$ and a neutral EgCG (Fig. 5). The ion retains the overall charge

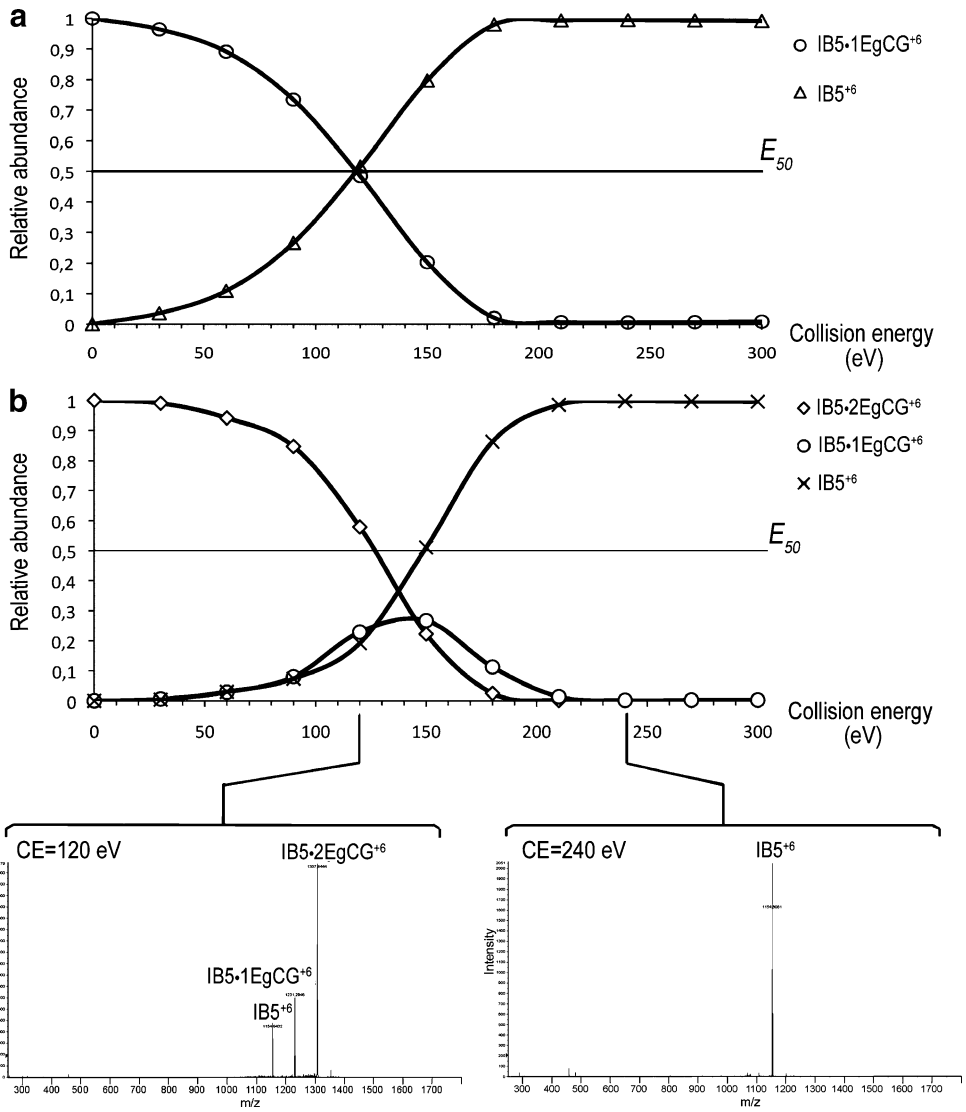

Fig. 5 **a** Plots of dissociation of $[IB5{\cdot}EgCG]^{6+}$ ion and appearance of the $[IB5]^{6+}$ ion. **b** Plots of dissociation of $[IB5{\cdot}2EgCG]^{6+}$ ion, appearance and dissociation of $[IB5{\cdot}EgCG]^{6+}$ ion, and appearance of the $[IB5]^{6+}$ ion. The *y*-axis represents relative abundance of ions; *insets* are CID-MS/MS spectrum of the selected $[IB5{\cdot}2EgCG]^{6+}$ complex ion (*m/z* 1,307) for collision energy 120 eV and collision energy 240 eV

as expected, whereas EgGC is released as a neutral species. Moreover, collision energy thresholds of total dissociation of [IB5·EgCG] and [IB5·2 EgCG] complex ions are 180 eV and 210 eV, respectively, showing the greater stability of the latter. Spectra obtained at CID lower collision energies allowed detection of both the remaining parent complex and $IB5^{6+}$ ions (Fig. 5a). In the case of 1:2 complexes, ions corresponding to the 1:1 complex are also detected. Precursor and product ions exhibit the same charge state (Fig. 5b). Thus, dissociation pathways for $[IB5{\cdot}2EgCG]^{6+}$ result from neutral loss of EgCG:

$$[IB5 \cdot 2EgCG]^{6+} \rightarrow [IB5 \cdot EgCG]^{6+} + EgCG$$
$$\rightarrow [IB5]^{6+} + 2EgCG$$

Table 2 Collision energy corresponding to 50% abundance of the precursor ions (E_{50}) in the laboratory frame (E_{Lab}) and in the center of mass (E_{CoM})

E_{50}(eV)	IB5·EgCG (1:1)	IB5·2EgCG (1:2)
E_{Lab}	120	127.5
E_{CoM}	0.45	0.45

Dissociation of the precursor complex ions leads to a decrease in stoichiometry down to the protein alone. Increasing energy on the parent ion releases the first tannin before the second one. Both tannins do not dissociate together from IB5. Nonetheless, this observation alone does not allow us to conclude whether tannins are bound on two different sites over IB5 or not.

Dissociation energies for $[IB5{\cdot}x\text{EgCG}]$ ions (x=1 or 2) were determined to give a measurement of the relative EgCG binding energies in these complexes. Relative abundance of the precursor ion was calculated as $I_p/(I_p + \sum I_{frag})$, where I_p is the peak intensity of the precursor ion,

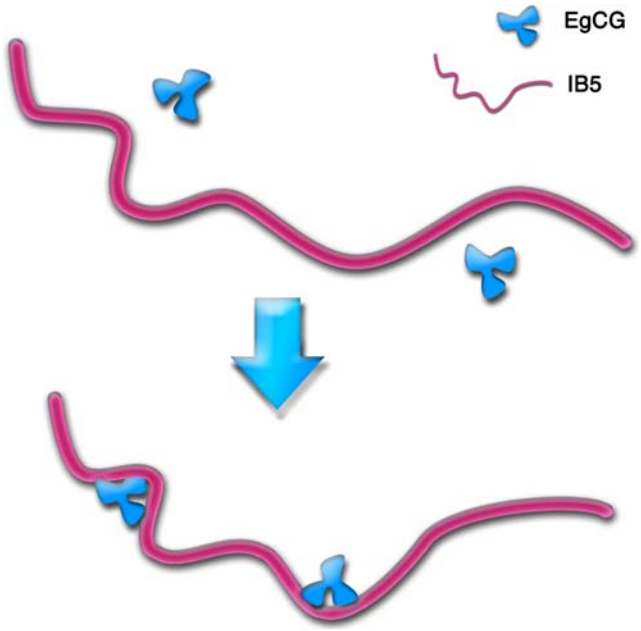

Fig. 6 Schematic illustrating the interaction between IB5 and EgCG

and $\sum I_{frag}$ is the sum of the peak intensities corresponding to all fragments [70]. This ratio is used to monitor the internal energy added to the complex ions to dissociate. The maximum energy that ions can acquire in the collision cell is the center-of-mass collision energy (E_{CoM}) of each collision summed over all. Laboratory frame collision energies (E_{Lab}) are converted to center-of-mass energies by using the equation

$$E_{CoM} = E_{Lab}\frac{m_g}{m_g + m_i} \quad (1)$$

where m_g and m_i are the mass of the target gas and of the complex ion, respectively.

The number of collisions (N_{col}) is determined by three parameters, the gas number density (n) , the length of the collision cell (l), and the collision cross section (σ) of the selected ion :

$$N_{col} = n \times \sigma \times l \quad (2)$$

Finally, the internal energy E_{Int} can be calculated from equation

$$E_{Int} = E_{CoM} \times N_{col} \quad (3)$$

As a first-order approximation, both complexes are expected to present very similar collision cross section because of the mere modification of their MM and their similar charge state [71]. Equation (2) shows that ions with similar cross section experience an identical number of collisions, thus from Eq. (3) their E_{Int} can be directly compared. From Eqs. (1) and (3), direct access to E_{Int} can be obtained via measurement of E_{CoM} for each species present in the spectrum. Moreover, previous works on proteins by the Douglas group provided evidence of the efficiency of energy transfer in a quadrupole, showing that almost 90% of the center-of-mass-energy is converted to internal energy [72]. Thus E_{Int} is approximately given by the center-of-mass energy E_{CoM} [72, 73]. For $[IB5{\cdot}EgCG]^{6+}$ and $[IB5{\cdot}2\ EgCG]^{6+}$ complex ions, dissociation curves as a function of collision energy were plotted, and the half-wave collision energy (E_{50}) was defined. E_{50} in the laboratory frame is the collision energy required to disrupt 50% of the parent complex ions. From the dissociation curves, E_{50} values have been established at 120 eV and 127.5 eV, respectively (Table 2). From these measurements, E_{50} in the center of mass (referred to as E_{CoM}) for $[IB5{\cdot}EgCG]^{6+}$ and $[IB5{\cdot}2\ EgCG]^{6+}$ ions are obtained (Table 2). The magnitude of that energy is related to the stability of the complex. Hence, we find that both $[IB5{\cdot}EgCG]^{6+}$ and $[IB5{\cdot}2\ EgCG]^{6+}$ ions (Table 2) have the same E_{CoM}. This implies that the same energy is required to either dissociate one EgCG from the IB5·2 EgCG complex or to dissociate the 1:1 complex. This feature highlights that EgCGs are involved within the complex with the same strength, indicating that they are bound on equivalent sites on IB5. These data support the presence of at least two potential equivalent interaction sites on IB5, as schematically illustrated in Fig. 6. Moreover, the intrinsic disorder of IB5 makes room for quite a large interaction surface, thus increasing the number of tannins that IB5 can bind [3].

Conclusions

Our experiments have demonstrated the ability of ESI-MS and ESI-MS/MS to detect and characterize noncovalent protein–polyphenol complexes with a charge state distribution similar to that of the protein alone. Direct access to the complex stoichiometry has been reached through ESI-MS analysis, where a maximum of 5 EgCG for 1 protein has been observed. For the first time, this approach affords an opportunity to estimate the ability of polyphenols to form soluble complexes with a protein different stoichiometry and to evaluate their stability. Our results indicate that IB5 possesses several interaction sites to bind tannins. In the light of both observed stoichiometries and IB5 sequence, the repeated motif “KPQGPP” could be the main site for interaction. This study confirms that the stability of protein–tannin complexes increases with the number of bound tannins and presumably with the number of repeated amino acid sequences [74]. Moreover, EgCG is likely to interact simultaneously through several sites of IB5. Another interesting consequence is that only PRP–tannin complexes made with full-length PRP sequences resist degradation under conditions such as encountered in

digestion [75]. This study is part of a general theme centered on the relevance of ESI-MS to probe protein–tannin solution-phase properties. Indeed, it clearly demonstrates that ESI-MS is well suited to detect associated polyphenols and will be used in further work to evaluate the ability of structurally distinguishable tannins to interact with peptides or proteins keeping in mind their astringency.

Acknowledgement The authors thank Hélène Boze and Claire Bouchut (UMR 1083 SPO) for their help in protein production and purification and MS experiments. We acknowledge synchrotron SOLEIL and thank all staff for assistance in using beamline DISCO. AG thanks Applied Biosystems (Les Ullis, France) for the loan of the IonCooler Guide. This work is supported by grant 07-BLAN-0279 from the French Agence Nationale de la Recherche (A.N.R.).

References

1. Tompa P (2002) Trends Biochem Sci 27:527–533
2. Dyson HJ, Wright PE (2005) Nat Rev Mol Cell Biol 6:197–208
3. Dunker AK, Brown CJ, Lawson JD, Iakoucheva LM, Obradovic Z (2002) Biochemistry 41:6573–6582
4. Bennick A (1982) Mol Cell Biochem 45:83–99
5. Robbins CT, Hagerman AE, Austin PJ, Arthur CM, Hanley TA (1991) J Mammal 72:480–486
6. Haslam E, Lilley TH, Cai Y, Martin R, Magnolato D (1989) Planta Med 55:v
7. McMurrough I, Madigan D, Kelly RJ, Smyth MR (1996) J Am Soc Brew Chem 54:141–148
8. McMurrough I, Hennigan GP, Loughrey MJ (1983) J Inst Brew 89:15–23
9. Waters EJ, Peng Z, Pocock KF, Williams PJ (1995) Aust J Grape Wine Res I:86–93
10. Butler LG (1992) In: Hemingway RW, Laks PE (eds) Antinutritional effects of condensed and hydrolyzable tannins. Plenum, New York
11. Dangles O (2006) Agro Food Ind Hi-Tech 17:64–67
12. van Valen L (1973) Evol Theory 1:1–30
13. Breslin PA, Gilmore M, Beauchamp GK, Green BG (1993) Chem Senses 18:405–417
14. Green BG (1993) Acta Psychol 84:119–125
15. Clifford MN (1997) In: Tomas-Barberan F, Robins R (eds) Astringency. Clarendon, Oxford
16. Noble A (1998) In: Waterhouse AL, Eberler S (eds) Why do wines taste bitter and feel astringent ? American Chemical Society, Washington
17. Hagerman AE (1989) In: Hemingway RW, Karchesy JJ (eds) Chemistry of tannin-protein complexation. Plenum, New York, London
18. Bate-Smith EC (1954) Food 23:124–135
19. Haslam E (1996) J Nat Prod 59:205–215
20. Simon C, Barathieu K, Laguerre M, Schmitter JM, Fouquet E, Pianet I, Dufourc EJ (2003) Biochemistry 42:10385–10395
21. Pascal C, Poncet-Legrand C, Imberty A, Gautier C, Sarni-Manchado P, Cheynier V, Vernhet A (2007) J Agric Food Chem 55:4895–4901
22. Sarni-Manchado P, Canals-Bosch J, Mazerolles G, Cheynier V (2008) J Agric Food Chem 56:9563–9569
23. Porter LJ, Woodruffe J (1984) Phytochemistry 23:1255–1256
24. Okuda T, Mori K, Hatano T (1985) Chem Pharm Bull 33:1424–1433
25. Baxter NJ, Lilley TH, Haslam E, Williamson MP (1997) Biochemistry 36:5566–5577
26. Hatano T, Hemingway RW (1996) J Chem Soc Chem Comm:2537–2538
27. Luck G, Liao H, Murray NJ, Grimmer HR, Warminski EE, Williamson MP, Lilley TH, Haslam E (1994) Phytochemistry 37:357–371
28. Murray NJ, Williamson MP, Lilley TH, Haslam E (1994) Eur J Biochem 219:923–935
29. Vergé S, Richard T, Moreau S, Nurich A, Merillon J-M, Vercauteren J, Monti J-P (2002) Biochim Biophys Acta 1571:89–101
30. Sarni-Manchado P, Cheynier V (2002) J Mass Spectrom 37:609–616
31. Vergé S, Richard T, Moreau S, Richelme-David S, Vercauteren J, Promé J-C, Monti J-P (2002) Tetrahedron Lett 43:2363–2366
32. Chen Y, Hagerman AE (2004) J Agric Food Chem 52:4008–4011
33. Loo JA, Sannes-Lowery KA (1997) Mass Spectrom Rev 16:1–23
34. Pramanik BN, Bartner PL, Mirza UA, Liu YH, Ganguly AK (1998) J Mass Spectrom 33:911–920
35. Jorgensen TJD, Roepstorff P, Heck AJR (1998) Anal Chem 70:4427–4432
36. Kapur A, Beck JL, Brown SE, Dixon NE, Sheil MM (2002) Protein Sci 11:147–157
37. Bligh SWA, Haley T, Lowe PN (2003) J Mol Recognit 16:139–148
38. Gupta R, Kapur A, Beck JL, Sheil MM (2001) Rapid Commun Mass Spectrom 15:2472–2480
39. de Brouwer APM, Versluis C, Westerman J, Roelofsen B, Heck AJR, Wirtz KWA (2002) Biochemistry 41:8013–8018
40. Benesch JLP, Sobott F, Robinson CV (2003) Anal Chem 75:2208–2214
41. Rosu F, De Pauw E, Gabelica V (2008) Biochimie 90:1074–1087
42. Pascal C, Bigey F, Ratomahenina R, Boze H, Moulin G, Sarni-Manchado P (2006) Protein Expr Purif 47:524–532
43. Yin S, Xie Y, Loo JA (2008) J Am Soc Mass Spectrom 19:1199–1208
44. Haller I, Mirza UA, Chait BT (1996) J Am Soc Mass Spectrom 7:677–681
45. Robinson CV (2001) J Am Soc Mass Spectrom 12:126–126
46. Zhang J, Kashket S (1998) Caries Res 32:233–238
47. Jørgensen TJD, Delforge D, Remacle J, Bojesen G, Roepstorff P (1999) Int J Mass Spectrom Ion Process 188:63–85
48. Wan KX, Gross ML, Shibue T (2000) J Am Soc Mass Spectrom 11:450–457
49. Akashi S, Osawa R, Nishimura Y (2005) J Am Soc Mass Spectrom 16:116–125
50. Harrison AG (1997) Mass Spectrom Rev 16:201–217
51. Bleiholder C, Suhai S, Paizs B (2006) J Am Soc Mass Spectrom 17:1275–1281
52. Yi SL, Boys BL, Brickenden A, Konermann L, Choy WY (2007) Biochemistry 46:13120–13130
53. Engel BJ, Pan P, Reid GE, Wells JM, McLuckey SA (2002) Int J Mass Spectrom Ion Process 219:171–187
54. Breci LA, Tabb DL III, JRY WVH (2003) Anal Chem 75:1963–1971
55. Vaisar T, Urban J (1996) J Mass Spectrom 31:1185–1187
56. Zhang X, Jai-nhuknan J, Cassady CJ (1997) Int J Mass Spectrom Ion Process 171:135–145
57. Leymarie N, Berg EA, McComb ME, O'Connor PB, Grogan J, Oppenheim FG, Costello CE (2002) Anal Chem 74:4124–4132
58. Flanzy C (1998) Oenologie — Fondements scientifiques et technologiques. Lavoisier, Paris
59. Sharon M, Robinson CV (2007) Annu Rev Biochem 76:167–193
60. Hagerman AE, Rice ME, Richard NT (1998) J Agric Food Chem 46:2590–2595
61. Poncet-Legrand C, Gautier C, Cheynier V, Imberty A (2007) J Agric Food Chem 55:9235–9240

62. Robinson CV, Chung EW, Kragelund BB, Knudsen J, Aplin RT, Poulsen FM, Dobson CM (1996) J Am Chem Soc 118:8646–8653
63. Sobott FM, Hernández H, McCammon MG, Robinson CV (2005) Phil Trans R Soc A 363:379–391
64. Mehansho H, Hagerman A, Clements S, Butler LG, Rogler JC, Carlson DM (1983) Proc Natl Acad Sci USA 80:3948–3952
65. Carlson DM (1993) Crit Rev Oral Biol Med 4:495–502
66. Sarni-Manchado P, Cheynier V, Moutounet M (1999) J Agric Food Chem 47:42–47
67. Tompa P (2003) J Mol Struc (Theochem) 361–371
68. Khalsa-Moyers G, McDonald WH (2006) Brief Funct Genomic Proteomic 5:98–111
69. Ruotolo BT, Robinson CV (2006) Curr Opin Chem Biol 10:402–408
70. Ham BM, Cole RB (2005) Anal Chem 77:4148–4159
71. Chen Y-LC, JM, Collings BA, Konermann L, Douglas DJ (1998) Rapid Commun Mass Spectrom 12:1003–1010
72. Chen Y-L, Collings BA, Douglas DJ (1997) J Am Soc Mass Spectrom 8:681–687
73. Wells JM, McLuckey SA (2005) In: Collision induced dissociation (CID) of peptides and proteins. Academic, New York
74. Charlton AJ, Baxter NJ, Lilley TH, Haslam E, McDonald CJ, Williamson MP (1996) FEBS Lett 382:289–292
75. Lu Y, Bennick A (1998) Arch Oral Biol 43:717–728